

# Accuracy of cloud liquid water path from ground-based microwave radiometry

## 1. Dependency on cloud model statistics

Ulrich Löhnert and Susanne Crewell

Meteorological Institute, University of Bonn, Bonn, Germany

Received 6 March 2002; revised 18 June 2002; accepted 21 August 2002; published 7 February 2003.

[1] This paper investigates the influence of cloud model statistics on the accuracy of statistical multiple-frequency liquid water path (LWP) retrievals for a ground-based microwave radiometer. Statistical algorithms were developed from a radiosonde data set in which clouds were modeled by using a relative humidity threshold and a modified adiabatic assumption. Evaluation of the algorithms was then performed by applying the algorithms to four data sets in which clouds were generated in different ways (i.e., threshold method, gradient method, and cloud microphysical model). While classical two-channel algorithms, in this case using frequencies at 22.985 and 28.235 GHz, do not show a significant dependency on the cloud model, the inclusion of an additional 50-GHz channel can introduce significant systematic errors. The addition of a 90-GHz frequency to the two-channel algorithm leads to a larger increase in LWP accuracy than in case of the 50-GHz channel and is less sensitive to the choice of cloud model. A drizzle case from the cloud microphysical model shows no significant loss of accuracy for the microwave radiometer algorithms, in contrast to simple cloud radar retrievals of liquid water. In case of rain, however, the results deteriorate when the total liquid water path is larger than  $700 \text{ g m}^{-2}$ .

**INDEX TERMS:** 3360 Meteorology and Atmospheric Dynamics: Remote sensing; 3394 Meteorology and Atmospheric Dynamics: Instruments and techniques; 6969 Radio Science: Remote sensing; 1640 Global Change: Remote sensing; 1655 Global Change: Water cycles (1836); **KEYWORDS:** microwave radiometer, cloud liquid water, sensor synergy, ground-based remote sensing

**Citation:** Löhnert, U., and S. Crewell, Accuracy of cloud liquid water path from ground-based microwave radiometry, 1, Dependency on cloud model statistics, *Radio Sci.*, 38(3), 8041, doi:10.1029/2002RS002654, 2003.

## 1. Introduction

[2] Clouds are still one of the major uncertainties in atmospheric models, whereby their role in linking radiation and dynamics is ill represented [e.g., Gates *et al.*, 1999]. Even thin clouds with small amounts of liquid water serve as effective radiation modulators and cause large changes in solar transmission. Thus, in order to describe the variability of solar transmission in numerical weather prediction and climate models in an adequate way, it is extremely important to develop instruments and retrieval algorithms which can observe cloud water, e.g., the prognostic variable describing clouds in atmospheric models, with the highest accuracy possible. For evaluation of model predicted cloud parameters long-term time series

need to be compared, as currently being done for the European BALTEX Cloud Liquid Water Network (CLIWA-NET) [Crewell *et al.*, 2002]. Principally, profiles of vertical cloud liquid water content (LWC) are needed for this purpose. Besides sporadic and expensive in-situ measurements from research aircraft, LWC can be derived from reflectivity factor ( $Z$ ) profiles measured by a cloud radar. However, due to the fact that LWC is proportional to the total volume of all cloud drops (drop radius cubed) and  $Z$  is proportional to the cloud drop radius to the order of six [e.g., Ulaby *et al.*, 1981], the conversion of  $Z$  to LWC can have an error of more than one order of magnitude.

[3] In comparison to cloud radars, microwave radiometers only have a very limited possibility to derive the vertical structure of cloud liquid. Since the inverse problem of deriving LWC profiles from microwave radiometer measurements is underdetermined, a large number of solutions for the atmospheric state can be found to satisfy each combination of measurements.

However, ground-based passive microwave remote sensing is by far the most accurate method to derive the vertical integral of LWC or the liquid water path (LWP). The high accuracy in retrieved LWP and integrated water vapor content (IWV) achieved by two-channel radiometers was demonstrated more than two decades ago [Westwater, 1978]. Together with their simple operation these reasons make microwave radiometers well suited to gather long-term time series needed for atmospheric model evaluation and improvement.

[4] Typically, the atmospheric brightness temperature (TB) is measured at one frequency on the wing of the water vapor line at 22.235 GHz and at a second frequency in the window region around 30 GHz (Figure 1). The first frequency is chosen so that the water vapor absorption coefficient is nearly independent of altitude. Because the emission of cloud liquid water increases with the frequency squared, the signal at the second frequency is dominated by liquid water contribution (Figure 1). From measurements at both frequencies LWP and IWV can be retrieved simultaneously.

[5] Recently, it has been suggested that LWP retrievals can be improved by adding a temperature-dependent frequency around 50 GHz [Bosisio and Mallet, 1998] or an additional frequency sensitive to cloud liquid water at 85 GHz [Bobak and Ruf, 2000]. Within this study we will compare LWP retrieval accuracies obtained with different frequency combinations obtained from the Microwave Radiometer for Cloud Cartography (MICCY) [Crewell *et al.*, 2001] of the University of Bonn.

[6] Existing LWP retrievals are often categorized into statistical and “physical” algorithms. Pure statistical algorithms are based on a set of concurrent TB and LWP values, which are related by some kind of function. The classical “physical” algorithm finds a solution for the profiles of temperature, humidity, and LWC such that the measured brightness temperatures are very close to the ones simulated from the derived profile of the atmospheric state [Peter and Kämpfer, 1992]. Since a large number of atmospheric states can satisfy each combination of TBs, constraints have to be chosen which will reduce the degrees of freedom. Therefore, many LWP retrievals are described as “physical,” but almost always depend on some sort of statistical assumptions about the atmospheric state, which are often site dependent [Han and Westwater, 1995]. Hence, statistical information of some sort always influences the retrieval. The statistics for atmospheric temperature and humidity are relatively well known from radiosonde measurements, but profiles of LWC are much more difficult to assess.

[7] To investigate the effect of insufficient knowledge of LWC statistics on LWP retrievals, we focus solely on pure statistical LWP retrievals. Up to now only very simple models to estimate the LWC profile from radiosonde measurements have been used. A common

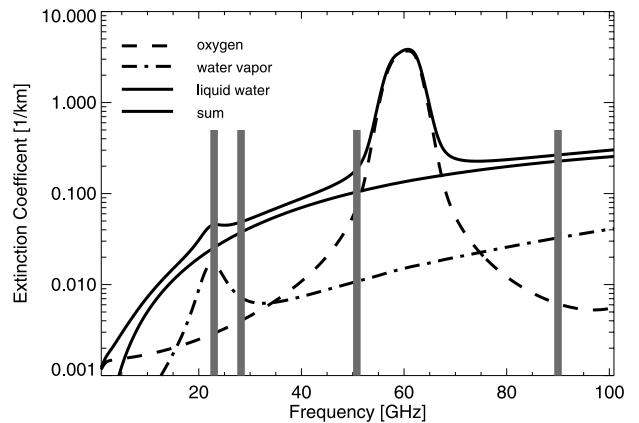


**Figure 1.** Microwave extinction due to water vapor, oxygen, and typical cloud liquid water content of  $0.2 \text{ g m}^{-3}$  at 895 hPa. The bars indicate the frequencies used for algorithm development in this study.

approach is to place clouds in a radiosonde profile, where the relative humidity exceeds a threshold of 95% (TH95). This method and three others, including one based on a microphysical cloud model, are presented in section 2 and are used to generate different cloud model testing data sets. In section 3 we describe the development of LWP retrieval algorithms, based on TH95, and regression techniques for inverting modeled TBs to LWP. In section 4 the algorithms are applied to the testing data sets and the significance of differences caused by the four different cloud models is investigated. The effects of larger drops within the atmosphere, i.e., drizzle and precipitation, on the retrieval results are shown in section 5. Finally, section 6 provides a summary of the results.

## 2. Cloud Liquid Water Profiles

[8] In this section we present three different methods to obtain representative data sets of LWC from radiosonde profiles. Within the development of retrieval algorithms TBs based on these LWC profiles are simulated to obtain relations between the TBs and LWP. Generally radiative transfer is drop size distribution (DSD) dependent in the microwave region, although DSD effects will only be significant at higher frequencies (90 GHz) or in rainy conditions. To be consequent, all radiative transfer calculations in this study are DSD-dependent and therefore scattering is calculated according to Mie theory for all clouds. The cloud DSDs are estimated as stated in section 2.1.

### 2.1. TH Methods

[9] Almost all efforts to diagnose LWC from radiosonde measurements use a threshold on relative humidity

(RH) [Wang *et al.*, 1999]. In this study LWC is set by 90% (TH90) and 95% (TH95) thresholds, i.e., cloud layers are taken to exist in a profile when RH exceeds the corresponding value. After determining the cloud boundaries, we calculate LWC from a modified adiabatic assumption [Karstens *et al.*, 1994]. Generally, the liquid water content as calculated for an adiabatic ascent (LWC<sub>ad</sub>), for example [Rogers and Yau, 1989], is assumed to be the maximum possible LWC and is corrected for effects of dry air entrainment, freezing drops or precipitation in the modified adiabatic approach. The empirical correction function used was derived from aircraft measurements of LWC in different types of clouds [Warner, 1955]:

$$\text{LWC} = \text{LWC}_{ad}(1.239 - 0.145 \ln(h)) \quad (1)$$

with  $h$  in m indicating the height above cloud base and  $h$  within the range between 1 and 5140 m.

[10] Size spectra for the derived LWC are described using the modified gamma distributions [Deirmendjian, 1969]:

$$n(r) = ar^\alpha \exp(-br^\gamma), \quad b = \frac{\alpha}{\gamma r_c^\gamma} \quad (2)$$

where  $r$  is the drop radius in  $\mu\text{m}$ ,  $n(r)$  is the drop density per unit increment of  $r$ ,  $r_c$  is the modal radius and  $a$ ,  $\alpha$ ,  $b$ , and  $\gamma$  were positive constants. Different distribution parameters are used for each cloud level depending on LWC (Table 1). Liquid water clouds were assumed down to temperatures of  $-20^\circ\text{C}$ .

## 2.2. CE Method

[11] An alternative approach for deriving cloud boundaries from radiosonde ascents is the gradient method proposed by Chernykh and Eskridge [1996] (in the following referred to as CE). A cloud is modeled into layers that satisfy the following conditions:

$$d^2T/dz^2 \geq 0, \quad d^2\text{RH}/dz^2 \leq 0, \quad (3)$$

with  $T$  denoting the temperature. These conditions can be interpreted as a region of a RH maximum due to saturation and a region of weaker temperature decrease within the cloud due to a pseudo-adiabatic lapse rate. After cloud boundary detection, Chernykh and Eskridge [1996] used a diagram according to Arabey [1975] to determine the dependency of cloud fraction on cloud temperature and dew point depression. Löhnert [1998] modified this diagram for the climatological conditions of Western Europe. Since the cloud models described above are one-dimensional, i.e., vertical profiles, cloud fraction cannot directly be taken into account. In order to consider cloud fraction, which can range from 0 to 100%, cloud fraction was interpreted as the probability of a cloud to exist above the measurement site.

**Table 1.** Drop-Size Distribution Parameters Related to the Modified Gamma Distribution Depending on LWC and Cloud Type<sup>a</sup>

Cloud Type	LWC, $\text{g m}^{-3}$	$r_c$ , $\mu\text{m}$	$\alpha$	$\gamma$	Author
<i>cu hum</i>	< 0.2	4.0	6.0	1.0	C1 Deirmendjian [1969]
<i>cu con</i>	0.2–0.4	6.0	4.0	1.0	C5 Deirmendjian [1975]
<i>Cb</i>	> 0.4	20.0	2.0	1.0	C6 Deirmendjian [1975]

<sup>a</sup>From Karstens *et al.* [1994].

Consequently, a random number between 0 and 100 was generated and compared with the modeled cloud fraction. If the random number was smaller than the modeled cloud fraction, a cloud is assumed to exist above the radiometer. The LWC profile is then calculated with the modified adiabatic method as described in section 2.1.

## 2.3. Dynamic Cloud Model

[12] In a further approach the 1.5-dimensional, micro-physical dynamic cloud model (DCM) of Issig [1997] is used. The DCM calculates LWC in 40 logarithmic radius classes every 250 m from ground to 10 km height (model top). This convective model was initialized with the radiosonde profiles that are also used for the static modeling in sections 2.1 and 2.2. Convection is initialized diabatically via a radiation module. This type of cloud modeling accounts for the temporal evolution of a typical cumulus cloud. Additionally, the derived temperature and humidity profiles are physically consistent with the LWC profile. However, the model always generates clouds, and hence, clear-sky cases are not well represented. A more detailed description of the model is given by Löhnert *et al.* [2001].

## 3. Retrieval Algorithm Development

### 3.1. Training Data Set

[13] The TH95 training data set, which is used for algorithm derivation, is based on a 5-year radiosonde data set consisting of the daily (0000 and 1200 UTC) ascents from the German Weather Service station Essen (located at  $51.5^\circ\text{N}$ ,  $7.0^\circ\text{E}$ ). The TH95 training data set exists only of LWP larger than  $30 \text{ g m}^{-2}$  and less than  $400 \text{ g m}^{-2}$ , thereby strictly encompassing only non-precipitating, cloudy cases. Many radiometer sites are equipped with additional instruments (e.g., infrared radiometers and ceilometers), so that the identification of cloud free scenes can be done independently. The value  $30 \text{ g m}^{-2}$  is chosen because it roughly represents the detection limit of LWP with two-channel radiometers [Crewell and Löhnert, 2003]. At LWP values larger than  $400 \text{ g m}^{-2}$  raindrops will occur and the

**Table 2.** The Number of Cases for All, Clear, Cloudy, and Rainy Conditions From the Data Sets TH95, TH90, CE and DCM<sup>a</sup>

	TH95	TH90	CE	DCM
Number cases (all)	4325	4325	4325	10104
Number of cloudy cases	1657	1577	1623	5947
Number of clear sky cases	1762	1211	2333	781
Number of rainy cases	906	1537	369	3376
LWP <sub>cloudy</sub> mean	170	187	143	195
LWP <sub>cloudy</sub> stddev	102	102	96	101
Number of cloud layers	1.32	1.33	1.32	1.12
Mean cloud thickness, km	0.810	0.828	0.742	1.209

<sup>a</sup>Clear, LWP < 30 g m<sup>-2</sup>; cloudy, 30 < LWP < 400 g m<sup>-2</sup>; rainy, LWP > 400 g m<sup>-2</sup>. Mean and standard deviation (stddev) of the LWPs from the cloudy data set (testing data set) are shown. Also shown are the average numbers of cloud layers and average cloud thickness of a single cloud layer. The latter two are calculated for cloudy cases only.

resulting brightness temperatures will become strongly drop size dependent especially at higher frequencies (e.g., 90 GHz).

### 3.2. Testing Data Sets

[14] In order to evaluate the algorithms, independent testing data sets are generated with the TH95, TH90, and CE cloud models using a second set of radiosonde data (Table 2). The number of cases (clear, cloudy, rainy) shown in Table 2 vary from model to model because different cloud models produce different percentages of rainy, clear and cloudy cases. To create the testing data sets for the TH95, TH90, and CE cloud models only the cases with LWP between 30 and 400 g m<sup>-2</sup> (cloudy cases, Table 2) are considered.

[15] A third set of radiosonde data is used to initialize the dynamic cloud model. After initialization, the model

is run for 2 hours with 40 s time resolution. To reduce the data volume, only those time steps that differ by more than 30 g m<sup>-2</sup> in LWP from the previous time step are used. Also only those time steps are considered, where LWP is between 30 and 400 g m<sup>-2</sup>. At each of these times, temperature, humidity, and LWC profiles are stored for the following radiative transfer.

[16] Among the static cloud models TH90 generates the most LWP and the thickest clouds due to the relatively low humidity threshold (Table 2). The CE model produces the most clear sky cases. Also, the CE model generates the smallest and the DCM model the largest LWPs mainly to the corresponding differences in cloud thickness.

[17] The mean vertical distributions of LWC for the testing data sets are shown in Figure 2. The mean DCM LWC profile (Figure 2a) and its standard deviation (Figure 2b) show a peak between 1.5 and 2 km, whereas the TH90 and TH95 models have a maximum roughly at 0.75 km. The CE model does not produce a dominant peak, but rather a more or less uniform distribution between 0.5 and 3.5 km, meaning that within this range CE clouds are equally probable at all heights.

### 3.3. Radiative Transfer

[18] The radiative transfer forward calculations are carried out with the microwave model MWMOD of *Simmer* [1994], which can simulate TBs in the range from 1 to 1000 GHz. The input parameters are atmospheric profiles of temperature, humidity, pressure, and hydrometeors. Gas absorption is calculated for oxygen and water vapor according to *Liebe et al.* [1993], while scattering and absorption due to hydrometeors are calculated using Mie theory. For all data sets TB calculations are carried out at 22.985, 28.235, 50.8,

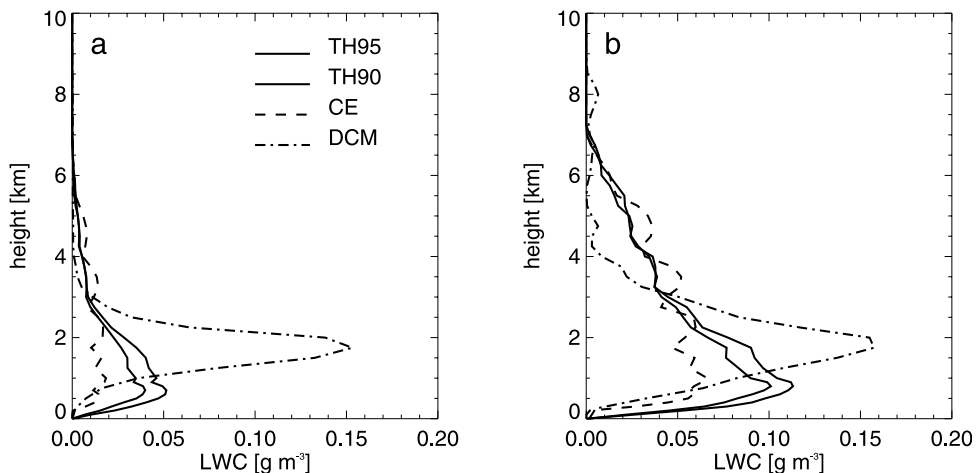


**Figure 2.** (a) Mean LWC profiles and (b) their standard deviations for the TH90, TH95, CE, and DCM cloud model testing data sets (only cloudy, nonraining cases).

and 90.0 GHz (Figure 1), which correspond to four channels of MICCY. The lower two channels represent the frequencies of the standard two-channel algorithm, and the 50.8- and 90-GHz channel represent distinct absorption properties used in prior studies. As shown by *Crewell and Löhnert* [2003], the use of more MICCY frequencies does not significantly increase the accuracy of LWP retrievals. All calculations and subsequent algorithm developments are performed at an elevation angle of 90°.

### 3.4. Regression Techniques

[19] In this section nine different LWP algorithms representing different input combinations are derived using the TH95 training data set. Only those cases with LWP between 30 and 400 g m<sup>-2</sup> are included in the retrieval algorithm development. A least squares linear regression model is applied to the training data pairs of **TB**/LWP. The size of the vector **TB** is varied according to the number of frequencies used in the retrieval. The general form of the linear retrieval can be written as

$$\text{LWP} = c_0 + \mathbf{c} \cdot \mathbf{TB} \quad (4)$$

with  $\mathbf{c}$  denoting the coefficient vector with dimension according to **TB**. The least squares regression minimizes

$$\chi^2 = \sum_k \left( \text{LWP}_k - c_0 - \sum_l c_l \text{TB}_{l,k} \right)^2 \quad (5)$$

with  $k$  denoting the number of **TB**/LWP pairs considered and  $l$  the dimension of **TB**. Minimization gives the optimal  $\mathbf{c}$  in the least squares sense as

$$\mathbf{c} = \mathbf{S}_{TB}^{-1} \mathbf{S}_{LWP, TB}, \quad (6)$$

with  $\mathbf{S}_{TB}$  denoting the covariance matrix of **TB** and  $\mathbf{S}_{LWP, TB}$  the vector of cross covariance between LWP and **TB**. Although LWP is the predictand and has no measurement error due to the synthetic generation by the cloud model, errors will occur due to the following reasons:

1. An arbitrary **TB** measurement relates to large number of atmospheric states.
2. Microwave radiative transfer within clouds cannot be fully described by a linear function.
3. Since we want to simulate the dependencies of actual **TB** measurements on LWP, Gaussian noise corresponding to the anticipated characteristics of MICCY (1 K for the lower three channels and 2 K for 90 GHz) was added to the **TBs**.

[20] Errors in radiative transfer and attenuation calculations will not affect the accuracies of LWP retrievals in this study since the algorithms are not applied to real measurements. The errors that can arise, e.g., due to

dependency on the gas absorption model used or due to calibration offsets, are described in detail by *Crewell and Löhnert* [2003].

[21] To account for possible nonlinearities the regression technique can be extended using quadratic terms of **TB**:

$$\text{LWP} = c_0 + \mathbf{c}_1 \cdot \mathbf{TB} + \mathbf{c}_2 \cdot \mathbf{TB}^2 \quad (7)$$

This retrieval will be compared to (4) in section 4 using different frequency combinations. A popular method for deriving LWP from a two-channel microwave radiometer is to use optical thickness ( $\tau$ ) instead of brightness temperature [*Westwater, 1978; Han and Westwater, 1995*] to account for nonlinearities.

$$\text{LWP} = d_0 + d_1 \tau_1 + d_2 \tau_2. \quad (8)$$

The optical thicknesses are commonly estimated from **TB** measurements via the so-called mean radiating temperature [*Hogg et al., 1983*], which is either estimated from the ground temperature or kept constant. The formulation of (8) can be derived from a simplified form of the radiative transfer equation where  $d_1$  and  $d_2$  can be calculated from the mean mass absorption coefficients of water vapor and liquid water. These in turn can usually be derived via regression from ground values of temperature, pressure and water vapor pressure, and are often left constant for reasons of simplicity. In this study a linear regression between LWP and  $\tau$  [*Güldner and Spänkuch, 1999*] was performed for comparison with the **TB** algorithms. Therefore, in total nine algorithms were developed and are listed in Table 3, which also provides the notation to distinguish both the frequency combinations and the use of pure linear (L) regression or inclusion of quadratic (Q) terms.

### 3.5. Application to the TH95 Training Data Set

[22] The accuracy of the LWP retrieval, when applied to the TH95 training data set used in algorithm development is shown in Table 3. As Table 3 shows, a large increase in accuracy can be gained from the addition of one or two channels to the standard two-channel algorithm. The 90-GHz channel is the most valuable when deriving LWP due to its high sensitivity to LWC. When all four channels are used, the RMS error between modeled and retrieved LWP is reduced by a factor of two. When regarding the relative explained variance defined as the square of the linear correlation coefficient ( $\text{COR}^2$ ) between modeled and retrieved LWP, roughly 12% of the LWP variance cannot be explained by the retrieval, whereas the four channel retrieval misses only 3% of the LWP variance. The inclusion of the quadratic terms for each frequency combination improves algorithm performance slightly. The regression using opac-

**Table 3.** The Different Algorithms and Frequencies Used in this Study<sup>a</sup>

Algorithm/Predictant	Frequencies, GHz	RMS, g m <sup>-2</sup>	COR <sup>2</sup>
L2/TB	22.985, 28.235	35.3	0.874
Q2/TB	22.985, 28.235, (22.985) <sup>2</sup> , (28.235) <sup>2</sup>	34.6	0.880
L2 (OT)/ $\tau$	22.985, 28.235	34.7	0.880
L3(90)/TB	22.985, 28.235, 90.0	19.8	0.960
Q3(90)/TB	22.985, 28.235, 90.0, (22.985) <sup>2</sup> , (28.235) <sup>2</sup> , (90.0) <sup>2</sup>	17.5	0.968
L3(50)/TB	22.985, 28.235, 50.8	22.4	0.951
Q3(50)/TB	22.985, 28.235, 50.8, (22.985) <sup>2</sup> , (28.235) <sup>2</sup> , (50.8) <sup>2</sup>	21.5	0.955
L4/TB	22.985, 28.235, 50.8, 90.0	17.4	0.970
Q4/TB	22.985, 28.235, 50.8, 90.0, (22.985) <sup>2</sup> , (28.235) <sup>2</sup> , (50.8) <sup>2</sup> , (90) <sup>2</sup>	15.4	0.976

<sup>a</sup>Also shown are the root mean square errors (RMS) and the squares of linear correlation (COR<sup>2</sup>) between modeled and retrieved LWP for each algorithm when applied to the TH95 training data set. The algorithms were applied to 1658 cases.

ities instead of TBs is about equivalent to the inclusion of quadratic terms for two frequencies (Q2).

## 4. Evaluation of Cloud Model Influence

[23] Each of the nine algorithms derived from the TH95 data set are now applied to the testing data sets derived from the TH95, TH90, CE, and DCM cloud models (cloudy, nonrainy cases only) in order to investigate retrieval sensitivity to cloud model statistics.

### 4.1. BIAS and RMS Errors

[24] The root mean square (RMS) and systematic (BIAS) errors of the different algorithms are illustrated in Figure 3. As expected, the RMS errors in Figure 3a show only minor deviations to the RMS values listed in Table 3. The RMS errors of the TH90 data set are very similar to the TH95 RMS, but a BIAS of about  $-5 \text{ g m}^{-2}$  occurs if only two frequencies are used. Note that with an increasing number of frequencies the systematic error decreases. The errors when applying the TH95 algorithm to the CE data set (Figure 3c) are dominated by systematic errors when using the 50.8 GHz channel information. The applications of L3(50) and Q3(50) result in a mean underestimation of LWP of about  $20 \text{ g m}^{-2}$ . This error is reduced significantly when the 90-GHz channel is used instead of the 50.8-GHz channel. For the L4 and Q4 retrieval algorithms, the underestimation effect can still be clearly seen. The RMS errors are slightly reduced for all four frequency combinations if the quadratic terms are used. The errors characteristic of the DCM testing data set (Figure 3d) are similar to those of the CE testing data set, but with the opposite sign for the systematic errors. The inclusion of 50.8 GHz as a third frequency again introduces a BIAS error in the range of  $17.5 \text{ g m}^{-2}$ , but in these cases a LWP overestimation occurs. For all four data sets the errors of the L2(OT) retrieval algorithm

do not differ significantly from the L2 and Q2 algorithm errors.

### 4.2. Relative Explained Variance

[25] The relative explained variance between model LWP and retrieved LWP is shown in Figure 4 for each retrieval algorithm and testing data set. Performance of the different retrieval algorithms applied to the testing data sets are now compared with COR<sup>2</sup> since COR<sup>2</sup> is independent both of the mean LWP and of the BIAS

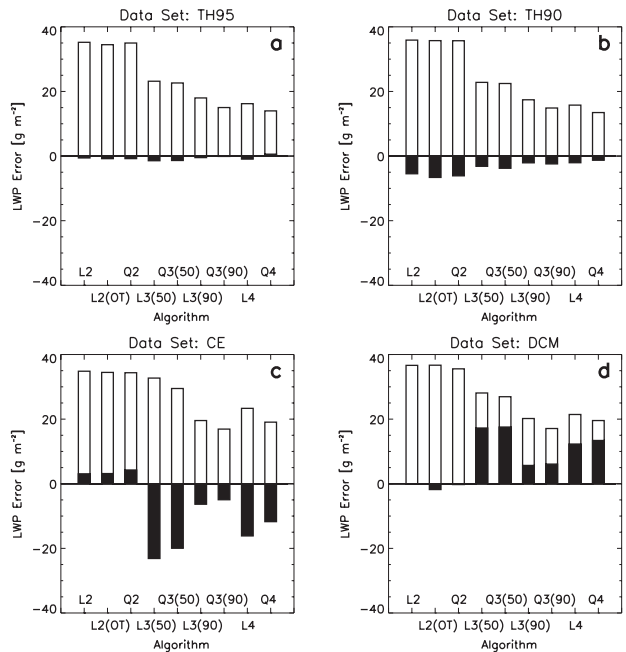


**Figure 3.** LWP RMS (nonshaded) and BIAS (dark shaded) errors of the nine algorithms applied to the different testing data sets.

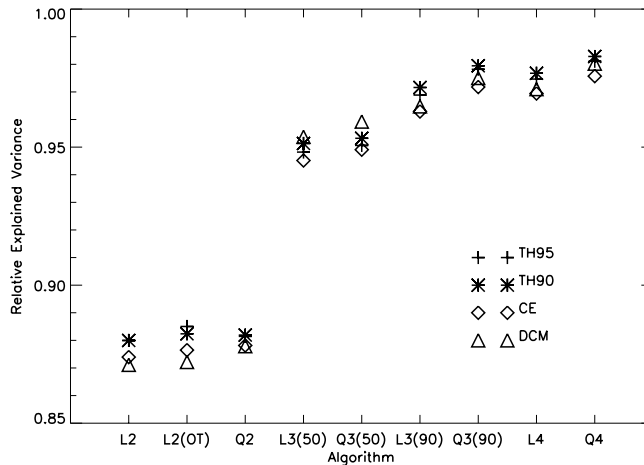


**Figure 4.** Relative explained variance between modeled and retrieved LWP in dependency of retrieval algorithm and cloud model testing data set.

error. The general (trivial) tendency shows that the inclusion of more channels increases the relative explained variance. The most significant improvement in  $COR^2$  is achieved when a third frequency is added to the two-frequency algorithm. In fact, the L3(90) and Q3(90) retrieval algorithms show higher values of  $COR^2$  than the L3(50) and Q3(50) algorithms. This result could also be seen when regarding  $COR^2$  in Table 3, only that now we can also verify this in a more general way.

[26] To interpret the results in Figure 4 a 99% confidence range ( $ci$ ) is calculated for each point in Figure 4 using the relationship

$$ci = COR \pm z_{\alpha}(1 - COR^2)/\sqrt{n - 1}, \quad (9)$$

with  $n$  denoting the number of cases and  $z_{\alpha}$  being the quantile of the standardized normal distribution corresponding to 99% (here 2.576 for the two-sided test). The  $ci$  denote the range in which the correlation coefficients of the universal population are to be expected. With this criterion all two-channel algorithms do not differ significantly with respect to the different data sets used. In comparison, some of the three- and four-channel retrievals show significant differences, especially when the  $COR$  derived from the CE data set is compared to  $COR$  from the other data sets. This result allows the conclusion that the two-channel algorithms do not depend as much on the data set (cloud model) used as the three- and four-channel algorithms.

### 4.3. Discussion on Error Sources

[27] Applying the TH95 algorithm to the CE and DCM data led to significant BIAS errors that dominated the error characteristics. Specifically, the 50.8-GHz channel

induced large BIAS errors if used in combination with the lower two channels. These errors arise due to differences in the mean LWPs of the different testing data sets (Table 2) and are therefore a statistical phenomenon.

[28] For the L3(50) algorithm applied to the CE data set, 82% of the retrieved LWP values are underestimated. These underestimations are due to lower TBs 80% of the time in the CE model compared with the corresponding TH95 TBs. The behavior of the BIAS error becomes clear from inspecting the derived regression coefficients (Figure 5). In case of L2 the effect of too low TBs is more or less compensated by the different signs of the L2 coefficients, but in the case of L3(50) this compensation will not work due to two positive coefficients and much higher values of the 50-GHz TB in comparison to the lower frequencies. This explains the negative BIAS of the L3(50) model. Although the 90-GHz channel is more sensitive to liquid water than the 50-GHz channel (i.e., the same amount of LWC increase leads to a larger TB increase at 90 GHz than at 50 GHz), the lower value of the third coefficient of L3(90) in comparison to the third coefficient of L3(50) makes L3(90) less sensitive to such a systematic error. A physical reason for this is the higher water vapor contribution at 90 GHz, which is even higher than at the center of the water vapor absorption line at 22.235 GHz (Figure 1), leading to a more indirect relationship between LWP and the 90-GHz channel. In fact, the correlation between LWP and the 90-GHz channel is 0.87, whereas the correlation between the 50.8-GHz channel and LWP is 0.90 for the TH95 testing data set. We can conclude that the 90-GHz channel complements the lower two channels better than the 50.8-GHz channel.

[29] In case of the DCM testing data set, TBs are generally higher than in the TH95 data set due to larger

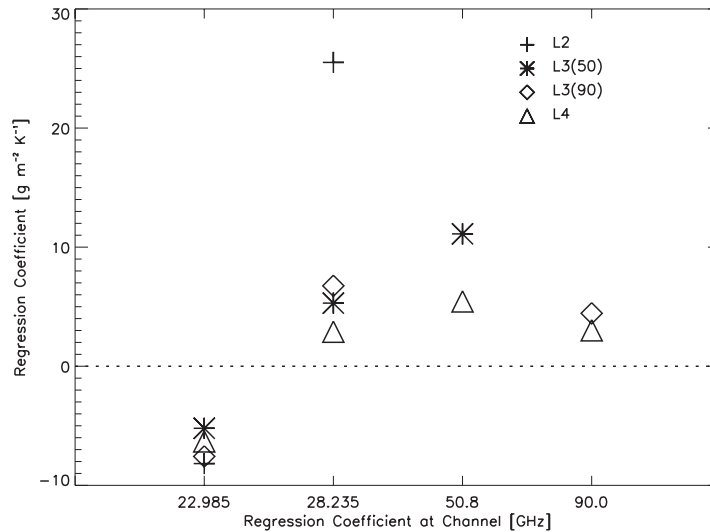


Figure 5. Derived regression coefficients for the algorithms L2, L3(50), L3(90), and L4.

LWPs, so that the same arguments are valid as for the CE data set, but with the opposite sign.

## 5. Effect of Precipitation

### 5.1. Influence of Drizzle

[30] The occurrence of drizzle particles can lead to large uncertainties when using cloud radar reflectivities alone to determine microphysical cloud properties [Fox and Illingworth, 1997]. Since microwave radiometers and cloud radars are often used in combination to infer LWC profiles from nonprecipitating clouds [Frisch et al., 1995; Löhnert et al., 2001], one must also need to know how sensitive microwave radiometer retrieval algorithms are to clouds containing moderate amounts of drizzle.

[31] In contrast to the three static cloud models (TH95, TH90, CE) the DCM calculates drop-size spectra throughout liquid clouds. These spectra can be used to identify drizzle cases, i.e., periods where larger drops with significant terminal velocities are present. In this study the size range of drizzle drops was set to radii from 50 to 400  $\mu\text{m}$  and drizzle water path (DWP) is defined as the liquid water path due to drops between 50 and 400  $\mu\text{m}$  in size. To test if the drizzle has any influence on the LWP retrieval, the DCM case with maximum DWP (32  $\text{g m}^{-2}$ ) is used as input to a modified version of MWMOD [Thiele, 2001] incorporating LWC drop-size spectra as specified by the DCM. As a consequence, brightness temperatures ( $\text{TB}_{\text{DSD}}$ ) could be simulated using the original spectra, instead of using a LWC-dependent gamma distribution as described in section 2.1.

[32] Application of the retrieval algorithms to  $\text{TB}_{\text{DSD}}$  (Figure 6) does not produce any significant differences in LWP ( $<2 \text{ g m}^{-2}$ ) compared to the results obtained from application to TBs generated by parametrized DSDs containing no drizzle droplets. Thus, moderate amounts of drizzle are not expected to have a significant impact on the accuracy of LWP retrievals and do not need to be considered when deriving algorithms. Also shown in Figure 6 is the LWP derived from radar reflectivities ( $Z$ ) using a standard  $Z$ -LWC relation. Here the drizzle droplets lead to an enormous overestimation of LWP, showing that cloud radar retrievals are extremely sensitive to drizzle. If the radar reflectivity is calculated without drizzle content (only contributions from drop

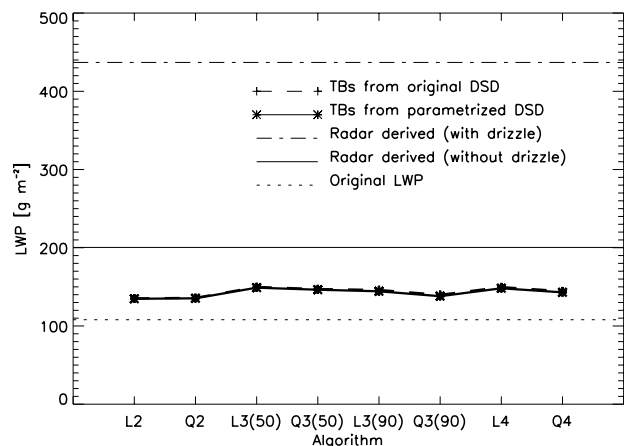


Figure 6. Impact on LWP retrieval when using an explicit DSD and a parametrized DSD to calculate TBs.

radii less than 50  $\mu\text{m}$ ) the cloud radar LWP retrieval is much more accurate.

## 5.2. Application to Raining Cases

[33] During continuous microwave radiometer observations of LWP it is important to discriminate between cloudy and rainy cases since rain will cause a diminished accuracy in LWP retrieval. *Czekala et al.* [2001] have proposed a method to discriminate rainwater from cloud liquid by polarized microwave radiometry. If polarimetric information is not available, discriminating light to moderate rain cases from cloudy cases is difficult, especially when the microwave radiometer is a stand-alone instrument without any additional rain screening information. Many times light rain will evaporate on its way to the ground. Rain may also be present, but not reach the radiometer, due to wind shear or a tilt in elevation of the radiometer. Considering these cases it is necessary to estimate how the TH95 algorithm performs during light to moderate rain cases since they cannot be completely filtered out. To test this sensitivity, rain is calculated for those cases of the TH95 cloud model data, where a LWP threshold of  $400 \text{ g m}^{-2}$  is exceeded. In this case an additional liquid water contribution is assumed, which is equally distributed as  $\text{LWC}_{\text{rain}}$  from the ground level to the freezing level [*Simmer, 1994*], defining the rainwater path (RWP), whereby the DSD of  $\text{LWC}_{\text{rain}}$  is modeled according to *Marschall and Palmer [1948]*. We will refer to the sum of the cloud water LWP and the additional RWP as total water path (TWP).

[34] In the following sensitivity study, 524 TH95 raining cases are used with TWP ranging from 400 to  $1000 \text{ g m}^{-2}$ . The BIAS and RMS errors that result for each retrieval algorithm are illustrated in Figure 7. The algo-

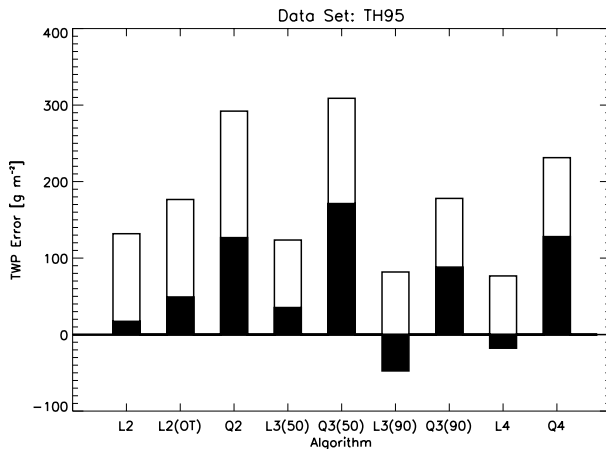


**Figure 7.** Total Water Path BIAS (dark shaded) and RMS (nonshaded) errors in dependency of algorithms for raining cases.

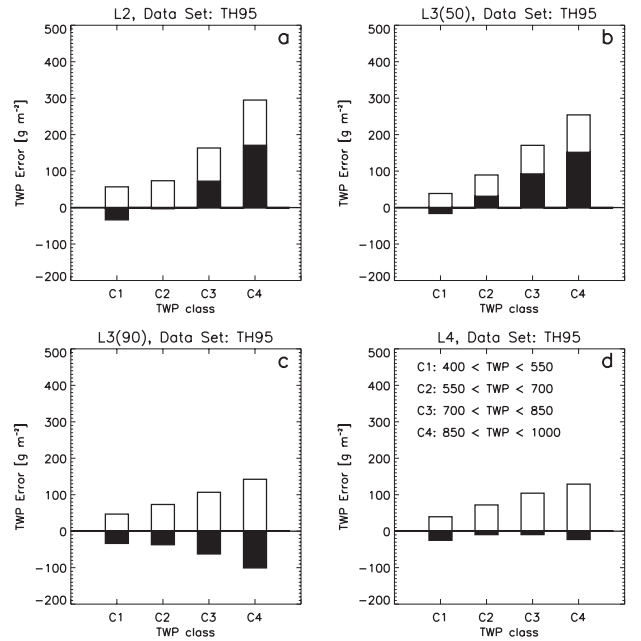


**Figure 8.** TWP BIAS (dark shaded) and RMS (nonshaded) errors for raining cases evaluated in four classes (C1, C2, C3, C4).

gorithms with quadratic terms of the brightness temperatures are now inaccurate, causing RMS errors up to  $300 \text{ g m}^{-2}$ , mainly caused by systematic overestimations.

[35] Since the errors of the linear algorithms are less dramatic, they are analyzed in more detail. As Figure 8 shows, the RMS and BIAS errors for these algorithms depend on the magnitude of TWP. The L2 and L3(50) retrievals show increasing positive BIAS errors with increasing TWP, whereas L3(90) shows increasing negative BIAS errors with increasing TWP. For the L4 algorithm compensating effects lead to much smaller errors. Since classes of low TWP values are not affected by large BIAS errors, overall errors are in the range of 15–20% for  $\text{TWP} < 700 \text{ g m}^{-2}$ . So, the retrieval algorithms might still be able to retrieve useful TWP values for values less than about  $700 \text{ g m}^{-2}$  even during rain cases. These error characteristics should not be generalized, since the algorithms are only applied to the TH95 data set and rain is only generated in one specific way as described in this section. A generalization would not only require different, independent data sets of TWP, but also different rain parametrizations, which go beyond the scope of this paper.

## 6. Conclusions

[36] For statistical LWP retrievals, RMS errors can be reduced by using an increasing number of frequencies. In

this study, the relative unexplained variance between “true” and retrieved LWP is reduced from 12% for a common two-channel algorithm to 3% for a four-channel algorithm. However, systematic errors due to different cloud model statistics become more significant as more channels are used. Specifically, when the 50.8-GHz channel is combined with the lower two channels, the algorithm accuracy depends very much on the cloud model used. In terms of LWP retrieval accuracy, the 90-GHz channel and the lower two channels complement one another better than the combination of the 50-GHz channel with the lower two channels. BIAS errors due to the different cloud model data sets are reduced and additionally the correlation between modeled and retrieved LWP is higher. Common two-channel algorithms are probably most suitable for climate effects, since they produce nearly BIAS free results. A statement of LWP accuracy for a certain retrieval algorithm containing statistical information should always be given in relation to the specific cloud model data set that was used to derive the retrieval algorithm.

[37] Different cloud models represent different possible states of the cloudy atmosphere. To best describe the universal state of the cloudy atmosphere, the cloud statistics used for algorithm development should contain a mixture of different statistics from different cloud models. Also, cloud data from 3-D cloud resolving models might help to create more representative statistics. The inclusion of physical constraints in the algorithm, e.g., including the consistency of the radiative transfer with the retrieved LWP or data from other remote sensing instruments (e.g., ceilometer, infrared radiometer, cloud radar) are strongly suggested.

[38] **Acknowledgments.** The authors would like to acknowledge Clemens Simmer and Harald Czekala from the University of Bonn for their fruitful contributions to this paper. We would also like to thank the German Weather Service for providing the radiosonde data.

## References

- Arabey, E. N., Radiosonde data as means for revealing cloud layers, *Meteorol. Gidrol.*, 6, 32–37, 1975.
- Bobak, J. P., and C. S. Ruf, Improvements and complications involved with adding an 85-GHz channel to cloud liquid water radiometers, *IEEE Trans. Geosci. Remote Sens.*, 38, 214–225, 2000.
- Bosisio, A. V., and C. Mallet, Influence of cloud temperature on brightness temperature and consequences for water retrieval, *Radio Sci.*, 33, 929–939, 1998.
- Chernykh, I. V., and R. E. Eskridge, Determination of cloud amount and level from radiosonde soundings, *J. Appl. Meteorol.*, 35, 1362–1369, 1996.
- Crewell, S., and V. Löhnert, Accuracy of cloud liquid water path from ground-based microwave radiometry, 2, Sensor accuracy and synergy, 108, doi:10.1029/2002RS002634, in press, 2003.
- Crewell, S., H. Czekala, U. Löhnert, T. Rose, C. Simmer, R. Zimmermann, and R. Zimmermann, Microwave radiometer for cloud cartography: A 22-channel ground-based microwave radiometer for atmospheric research, *Radio Sci.*, 36, 621–638, 2001.
- Crewell, S., M. Drusch, E. van Meijgaard, and A. van Lammeren, Cloud observation and modelling within the European BALTEX Cloud Liquid Water Network, *Boreal Environ. Res.*, 7, 235–245, 2002.
- Czekala, H., S. Crewell, C. Simmer, and A. Thiele, Discrimination of cloud and rain liquid water path by ground-based polarized microwave radiometry, *Geophys. Res. Lett.*, 28, 267–270, 2001.
- Deirmendjian, D., *Electromagnetic Scattering on Spherical Polydispersions*, 290 pp., Elsevier Sci., New York, 1969.
- Deirmendjian, D., Far-infrared and submillimeter wave attenuation by clouds and rain, *J. Appl. Meteorol.*, 14, 1584–1593, 1975.
- Fox, N., and A. J. Illingworth, The potential of spaceborn cloud radar for the detection of stratocumulus clouds, *J. Appl. Meteorol.*, 36, 485–492, 1997.
- Frisch, A. S., C. W. Fairall, and J. B. Snider, Measurement of stratus clouds and drizzle parameters in ASTEX with a Ka-band Doppler radar and a microwave radiometer, *J. Atmos. Sci.*, 52, 2788–2799, 1995.
- Gates, W. L., et al., An overview of the results of the atmospheric model intercomparison project (AMIP I), *Bull. Am. Meteorol. Soc.*, 80, 29–55, 1999.
- Güldner, J., and D. Spänkuch, Results of year-round remotely sensed integrated water vapor by ground-based microwave radiometry, *J. Appl. Meteorol.*, 38, 981–988, 1999.
- Han, Y., and E. Westwater, Remote sensing of tropospheric water vapor and cloud liquid water by integrated ground-based sensors, *J. Atmos. Oceanic Technol.*, 12, 1050–1059, 1995.
- Hogg, D. C., F. O. Guiraud, J. B. Snider, M. T. Decker, and E. R. Westwater, A steerable dual-channel microwave radiometer for measurement of water vapor and liquid in the troposphere, *J. Clim. Appl. Meteorol.*, 22, 789–806, 1983.
- Issig, C., *Ein spektrales Wolkenmodell mit integriertem Strahlungsübertragungsmodell zur Unterstützung von Niederschlagsalgorithmen*, Ph.D. thesis, Meteorol. Inst., Univ. of Bonn, Bonn, Germany, 1997.
- Karstens, U., C. Simmer, and E. Ruprecht, Remote sensing of cloud liquid water, *Meteorol. Atmos. Phys.*, 54, 157–171, 1994.
- Liebe, H. J., G. A. Hufford, and M. G. Cotton, Propagation modelling of moist air and suspended water/ice particles at frequencies below 1000 GHz, in *Proceedings AGARD 52nd Specialists Meeting of the Electromagnetic Wave Propagation Panel*, pp. 3-1–3-10, AGARD, Palma de Mallorca, Spain, 1993.

- Löhnert, U., *Bestimmung von Gesamtwasserdampf und Gesamtwolkenwasser anhand von PAMIR-Messungen in Bonn*, diploma thesis, Meteorol. Inst., Univ. of Bonn, Bonn, Germany, 1998.
- Löhnert, U., S. Crewell, A. Macke, and C. Simmer, Profiling cloud liquid water by combining active and passive microwave measurements with cloud model statistics, *J. Atmos. Oceanic Technol.*, 18, 1354–1366, 2001.
- Marschall, J. S., and W. K. Palmer, The distribution of raindrops with size, *J. Meteorol.*, 5, 165–166, 1948.
- Peter, R., and N. Kämpfer, Radiometric determination of water vapor and liquid water and its validation with other techniques, *J. Geophys. Res.*, 97, 18,173–18,183, 1992.
- Rogers, R. R., and M. K. Yau, *A Short Course in Cloud Physics*, 290 pp., Butterworth-Heinemann, Woburn, Mass., 1989.
- Simmer, C., *Satellitenfernerkundung Hydrologischer Parameter der Atmosphäre mit Mikrowellen*, 314 pp., Dr. Kovac, Hamburg, 1994.
- Thiele, A., *Einfluss des Polarisations signals von Mikrowellenstrahlung auf bodengebundene Fernerkundung von Wolken und Niederschlagswasser*, diploma thesis, Meteorol. Inst., Univ. of Bonn, Bonn, Germany, 2001.
- Ulaby, F. T., R. K. Moore, and A. D. Fung, *Microwave Remote Sensing Active and Passive*, vol. 1, 456 pp., Artech House, Norwood, Mass., 1981.
- Wang, J., W. B. Rossow, T. Uttal, and M. Rozendaal, Variability of cloud vertical structure during ASTEX observed from a combination of rawinsonde, radar, ceilometer, and satellite, *Mon. Weather Rev.*, 127, 2484–2502, 1999.
- Warner, J., The water content of cumuliform clouds, *Tellus*, 7, 449–457, 1955.
- Westwater, E., The accuracy of water vapor and cloud liquid determination by dual-frequency ground-based microwave radiometry, *Radio Sci.*, 13, 667–685, 1978.
- 
- S. Crewell and U. Löhnert, Meteorologisches Institut der Universität Bonn, Auf dem Hügel 20, 53121 Bonn, Germany. (uloeh@uni-bonn.de)